Cerebral Cortex January 2015;25:236–245
doi:10.1093/cercor/bht218
Advance Access publication August 21, 2013

Risk-Taking Behavior: Dopamine D2/D3 Receptors, Feedback, and Frontolimbic Activity

Milky Kohno[1,2], Dara G. Ghahremani[1], Angelica M. Morales[1,2], Chelsea L. Robertson[3,6], Kenji Ishibashi[1,6], Andrew T. Morgan[1,6], Mark A. Mandelkern[6,7] and Edythe D. London[1,2,3,4,5,6]

[1]Department of Psychiatry and Biobehavioral Sciences, [2]Neuroscience Interdepartmental Program, [3]Department of Molecular and Medical Pharmacology, [4]Brain Research Institute, University of California Los Angeles, [5]University of California Los Angeles Semel Institute, Los Angeles, CA 90024, USA and [6]Veterans Administration of Greater Los Angeles Healthcare System, [7]Department of Physics, University of California Irvine, Irvine, CA, USA

Address correspondence to Edythe D. London, University of California Los Angeles Semel Institute, 740 Westwood Plaza, C8-831, Los Angeles, CA 90024, USA. Email: elondon@mednet.ucla.edu

Decision-making involves frontolimbic and dopaminergic brain regions, but how prior choice outcomes, dopamine neurotransmission, and frontostriatal activity are integrated to affect choices is unclear. We tested 60 healthy volunteers using the Balloon Analogue Risk Task (BART) during functional magnetic resonance imaging. In the BART, participants can pump virtual balloons to increase potential monetary reward or cash out to receive accumulated reward; each pump presents greater risk and potential reward (represented by the pump number). In a separate session, we measured striatal D2/D3 dopamine receptor binding potential (BP_{ND}) with positron emission tomography in 13 of the participants. Losses were followed by fewer risky choices than wins; and during risk-taking after loss, amygdala and hippocampal activation exhibited greater modulation by pump number than after a cash-out event. Striatal D2/D3 BP_{ND} was positively related to the modulation of ventral striatal activation when participants decided to cash out and negatively to the number of pumps in the subsequent trial; but negatively related to the modulation of prefrontal cortical activation by pump number when participants took risk, and to overall earnings. These findings provide in vivo evidence for a potential mechanism by which dopaminergic neurotransmission may modulate risk-taking behavior through an interactive system of frontal and striatal activity.

Keywords: decision-making, dopamine receptors, fMRI, pet, risk-taking, striatum

Introduction

Decision-making under risky conditions can be crucial for survival, but how contextual information and brain processes are integrated to influence decisions is incompletely understood. Neuroimaging studies show frontostriatal activation during risky decision-making (Ernst and Paulus 2005; Krain et al. 2006; Rao et al. 2008). Moreover, while experience-dependent fluctuations in neural activation likely influence risky decision-making (Gold and Shadlen 2007; Dayan and Daw 2008; Niv et al. 2012), the precise relationships between brain activation during risky decision-making and its neurochemical correlates in the context of recent outcomes are relatively underexplored. We aimed to help clarify these relationships using positron emission tomography (PET) and functional magnetic resonance imaging (fMRI) paired with the Balloon Analogue Risk Task (BART; Lejuez et al. 2002). The BART presents sequential choices—pumping a virtual balloon to increase potential gains while risking loss if the balloon explodes, or cashing out and avoiding explosion. We used a parametric fMRI design to study how an increase in risk and potential reward (represented by pump number in a trial) modulated brain activation during decision-making.

Because activity in dopaminergic neurons increases with the magnitude of anticipated rewards (Tobler et al. 2005), and reward induces dopamine release and activation in the nucleus accumbens (Schott et al. 2008), we hypothesized that activation in the ventral striatum during cash-out events would be positively correlated with a dopaminergic marker. Notably, a recent study has shown that allelic variants of variable number tandem repeat polymorphism of the dopamine transporter gene (DAT1) influence risk-taking (Mata et al. 2012). Here, we determined D2/D3 dopamine-receptor availability, as binding potential (BP_{ND}), using [^{18}F]fallypride and PET in a subset of the participants who underwent fMRI. As D2/D3 receptor–agonist administration attenuates risk-taking in rodents (Simon et al. 2011), we expected that modulation of ventral striatal activation by pump number during cashing out would predict risk-taking in subsequent trials, and that this relationship would reflect variation in striatal BP_{ND}.

Responses to rewards may influence decision-making by maintaining a balance between reward-seeking, initiated by activity in the ventral striatum (Schultz 1998), and goal-directed behavior, guided by the prefrontal cortex (PFC) (Ridderinkhof et al. 2004). Observations that patients with PFC lesions have difficulty resisting immediate rewards at the expense of larger, future rewards suggest that the PFC regulates reward-seeking behavior (Bechara et al. 1998). In this regard, signaling through corticostriatal pathways may facilitate adaptive decision-making through PFC inhibition of ventral striatal activity. We therefore expected that striatal D2/D3 BP_{ND} would be inversely related to the modulation of PFC activation by pump number when participants took risk and also inversely related to overall monetary gain.

We also examined how the outcome of the previous trial is associated with subsequent risky decision-making by comparing the effects of losses and gains on risk-taking and associated neural activation. Because the inclination to avoid loss is greater than the preference to acquire reward (Kahneman and Tversky 1984), we expected that recent losses would attenuate risk-taking, and that behavioral effects would be related to activity in the insula and amygdala, regions that have been linked to negative affect (Berntson et al. 2011).

Materials and Methods

Participants

A total of 60 healthy, right-handed research volunteers (18–51 years of age; 27 females) participated in this study. They were recruited for

2 separate projects that were approved by the UCLA Office of the Human Research Protection Program. In both studies, participants performed the BART during fMRI using identical procedures. In one study, participants had the option of undergoing PET to assess dopamine D2/D3 receptor BP_{ND}. Sixty participants performed the BART during fMRI, and a subset of these participants ($n = 13$) had PET scans as well for the determination of D2/D3 receptor BP_{ND}. Exclusion criteria, determined by a physical examination and psychiatric evaluation using the Structured Clinical Interview for DSM-IV, were: Systemic, neurological, cardiovascular, or pulmonary disease; head trauma with loss of consciousness; any current Axis I psychiatric diagnoses except nicotine dependence; and current use of prescribed psychotropic medications. Participants who tested positive for cocaine, marijuana, methamphetamine, benzodiazepines, or opiates by urinalysis were excluded, as were those with MRI contraindications.

Balloon Analogue Risk Task

A version of the BART (Lejuez et al. 2002), adapted for event-related fMRI, was used (Fig. 1). Balloons were either red or blue on active trials and white on control trials. When presented with an active balloon, participants selected between pumping the balloon for a potential increase in earnings ($0.25/pump) or cashing out to retain earnings accumulated during that trial. Pumping increased the size of the balloon and accumulated earnings, or it resulted in balloon explosion and forfeiture of unrealized earnings accumulated during the trial. Trials included all pumps starting with the first presentation of a balloon and ended with the choice to cash out, which resulted in a 2-s display of the total earned, or in a balloon explosion followed by a 2-s display of an exploded balloon with the message, "Total = $0.00." Prior to scanning, participants were informed that red and blue balloons were associated with monetary reward and that they would receive their winnings after scanning, but not that the number of pumps that would produce an explosion was predetermined. For each active balloon trial, that number was determined from a uniform probability distribution, ranging from 1 to 8 and 1 to 12 pumps for red and blue balloons, respectively. Participants were informed that the white balloons did not explode and were not associated with potential reward, and they were instructed to pump each white balloon until the trial ended. The white-balloon trials were used to control for motor- and visual-related activation. The number of white-balloon presentations within the trial varied randomly between 1 and 12 ($M = 6.34$, SD = 3.44), according to a uniform distribution. Red, blue, and white-balloon trials were randomly interspersed throughout the task. The task was administered in two 10-min runs. As the task was self-paced and each balloon remained on the screen until the participant pressed a button, the duration of pump events varied with the participant, as did the total number of trials (active trials: $M = 56.62$, SD = 8.47; control trials: $M = 11.40$, SD = 2.39). Participants were able to cash out at any time prior to a balloon explosion, and the number of pumps within a trial varied with the participant (number of pumps on trials ending with the choice to cash out: $M = 2.92$, SD = 0.934; number of pumps on all active trials: $M = 8.48$, SD = 2.29). The interstimulus interval for balloon presentations was randomly sampled from a uniform distribution ranging from 1 to 3 s, and the intertrial interval was randomly sampled from an exponential distribution (mean: 4 s; range: 1–14 s). Participants received their earnings in cash at the end of the scanning session.

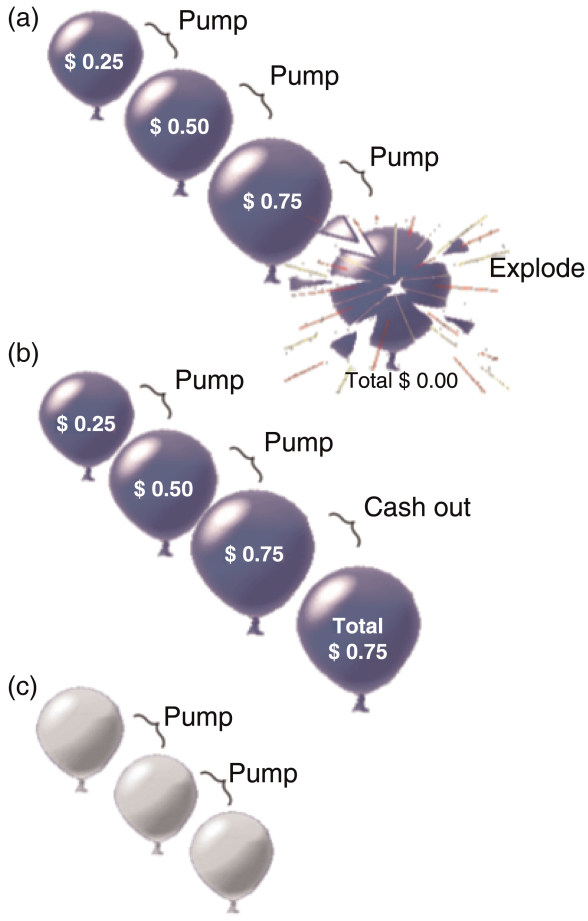

Figure 1. Balloon Analogue Risk Task. (*a*) Pumping the balloon increased potential earnings but carried the risk of the balloon exploding, resulting in a loss of accumulated earnings during the trial. (*b*) If participants cashed out before the balloon exploded, they retained the earnings accumulated. (*c*) In control trials, white balloons were presented. These balloons did not increase in size with pumping, did not explode, and were not associated with reward potential (see Methods).

fMRI Scanning

Imaging was performed at 3 T on a Siemens Magnetom Trio MRI system. A set of 302 functional, T_2*-weighted, echoplanar images (EPIs) were acquired (slice thickness = 4 mm; 34 slices; repetition time = 2 s; echo time = 30 ms; flip angle = 90°; matrix = 64 × 64; field of view = 200 mm). High-resolution, T_2-weighted, matched-bandwidth, and magnetization-prepared rapid-acquisition gradient echo (MPRAGE) scans were also acquired. The orientation for matched-bandwidth and EPI scans was oblique axial to maximize brain coverage and to optimize signal from ventromedial prefrontal regions.

PET Scanning

Dopamine D2/D3 receptor BP_{ND} was assayed using [^{18}F]fallypride, a high-affinity radioligand for dopamine D2/D3 receptors (Mukherjee et al. 1995). Images were acquired using a Siemens ECAT EXACT HR+ scanner [in-plane resolution full-width at half-maximum (FWHM) 4.6 mm, axial FWHM = 3.5 mm, axial field of view = 15.52 cm] in a 3-dimensional mode. A 7-min transmission scan was acquired using a rotating ^{68}Ge/^{68}Ga rod source for attenuation correction. PET dynamic data acquisition was initiated with a bolus injection of [^{18}F]fallypride (~5 mCi in 30 s). To minimize discomfort and to reduce radiation exposure to the bladder wall, emission data were acquired in two 80-min sessions separated by a break. Data were reconstructed using ECAT v7.3 OSEM (Ordered Subset Expectation Maximization; 3 iterations, 16 subsets) after corrections for decay, attenuation, and scatter.

Analysis of Behavioral Data

A general linear mixed model was used to examine risk-taking behavior while simultaneously modeling trial-by-trial data and taking into account individual subject variables. As trials progressed, risk-taking behavior may have been confounded by learning as participants received feedback reflecting the probabilities associated with the explosion of red and blue balloons. We therefore included the trial number (continuing across the 2 fMRI runs) and balloon color (red vs. blue balloons) into the model to examine the effect of learning on pumping during the trial. As our main analysis concerned the effects of recent experience on subsequent behavior, the outcome of the immediately preceding trial was also included in the model with pumps per trial as the dependent variable.

The general linear mixed model allows the inclusion of both trial-level and subject-level covariates and accounts for the nonindependence of observations clustered within subjects, and as such is a reasonable approach for the analysis of the BART where these types of covariates may influence results. It is also robust to missing data or to the exclusion of data, such as the outcome of white-balloon trials and pumping behavior on trials following white-balloon trials. The resulting estimates are valid and unbiased by missing or excluded observations, provided that the model accounts for factors associated with the pattern of exclusion (Laird 1988; Little and Rubin 2002; Fitzmaurice et al. 2004). That is, the case here since the white control balloons were not associated with monetary outcome and did not explode, but were fully modeled. Data were analyzed using the Statistical Package for the Social Sciences.

Analysis of fMRI Data

Image analysis was performed using the FMRIB Software Library (FSL; version 4.1.8; www.fmrib.ox.ac.uk/fsl). The image series from each participant was first realigned to compensate for small head movements (Jenkinson et al. 2002), and then a high-pass temporal filtering (100 s) was applied. Data were spatially smoothed using a 5-mm FWHM Gaussian kernel, and skull stripping was performed using the FSL Brain Extraction Tool. Registration was conducted through a 3-step procedure, whereby EPI images were first registered to the matched-bandwidth structural image, then to the high-resolution MPRAGE structural image, and finally into standard Montreal Neurological Institute space, using 12-parameter affine transformations. Registration of MPRAGE structural images to standard space was further refined using FNIRT nonlinear registration (Andersson et al. 2007). Statistical analyses were performed on data in native space using the FMRIB's fMRI Expert Analysis Tool (FEAT), and the statistical maps were spatially normalized to standard space prior to higher-level analysis.

Four types of events were included in the general linear model (GLM): Pumps on active balloons, cash outs, balloon explosions, and pumps on control balloons. Active-balloon and control-balloon pump events were defined as starting with the onset of the balloon presentation and ending with the button press to pump. Cash-out events were defined as the time between the appearance of the balloon and the disappearance of the feedback message, giving the total earned. Balloon explosion events started with the appearance of the exploded balloon and ended with the message "Total Earned = $0.00." As a trial progressed, risk and potential reward increased with each pump, as did the amount earned with the choice to cash out. For each of the 4 types of events, estimates of mean activation and of parametric modulation of activation (Buchel et al. 1998) by pump number were included in a GLM using FEAT. Parametric regressors tested the linear relationship between pump number and blood oxygen-level dependent (BOLD) signal, by using demeaned pump number (pump number minus the total number of pumps within each trial) as a parametric modulator with greater weight assigned to later pumps. For example, within a trial, the second pump event, for which greater reward was at stake, was given greater weight than the first. The parametric modulator for cash out and explode events was the number of pumps before the decision to cash out or before the balloon exploded, respectively. To maximize statistical power to conduct a more robust test for a linear relationship between level of risk and brain activation, red and blue balloons were combined. The nonparametric regressors were used to estimate the mean response for each event without consideration of the escalation of potential reward/loss within the trial.

Regressors were created by convolving a set of delta functions that represented the onset times of the events with a canonical (double-gamma) hemodynamic response function (HRF). The participant's response time to pump and the interstimulus interval determined the width of the HRF for each event. To allow for the separation of responses of the cash-out or balloon-explosion event from the final pump that preceded it, the width of the HRF for the last pump of each trial was modeled using the participant's response time. Additional regressors that represented the first temporal derivatives of the 8 event-related regressors were included to capture variance associated with slight variations in the temporal lag of the hemodynamic response.

Whole-brain statistical analyses, using a fixed-effects model, were conducted separately for each imaging run per participant, and again to combine contrast images across the 2 runs. For between-participant analyses, the FMRIB Local Analysis of Mixed-Effects module was used with sex and age as covariates. Statistical images were thresholded at a voxel height of $Z > 2.3$ and a cluster-probability threshold of $P < 0.05$, corrected for whole-brain multiple comparisons using the Theory of Gaussian Random Fields. Parameter estimates (β-values from the whole-brain GLM parametric analysis, corresponding to the modulation of activation by pump number) from a priori regions were extracted and used for subsequent correlation analyses with BART performance and striatal D2/D3 BP_{ND} (see below).

Effects of the Outcome of the Preceding Trial

A separate GLM was used to examine the effects of the outcome of the previous trial on the modulation of activation by pump number. For each participant, pump events in a trial were categorized on the basis of the outcome of the previous trial. The GLM included parametric and nonparametric regressors separately for pumps that followed cash outs, balloon explosions, control balloon trials, and the first trial of each run (with no preceding contextual outcome). The contrast of interest was: "Pumps Following a Cash Out versus Pumps Following a Balloon Explosion" (parametric regressors). The analysis was performed using a voxel-height threshold of $Z > 2.3$ and a cluster-probability threshold of $P < 0.05$, corrected for whole-brain multiple comparisons.

Analysis of PET Data

Reconstructed PET data were combined into 16 images, each containing an average of 10-min dynamic frames. PET images were corrected for head motion by aligning the other 15 images to the second image in the series using rigid-body transformation with FSL FLIRT. Coregistration of the second PET image to the structural MRI using the ART software package was computed using a 6-parameter, rigid-body transformation and was subsequently applied to all 16 PET images in the series (Ardekani et al. 1995). Bilateral caudate, putamen, and nucleus accumbens regions were defined on the participant's MPRAGE using FSL FIRST (http://www.fmrib.ox.ac.uk/fsl/first/index.html).

Time-radioactivity data from the caudate, putamen, and nucleus accumbens were extracted from the motion-corrected, coregistered images and imported into the PMOD 3.2 for kinetic modeling (PMOD Technologies Ltd., Zurich, Switzerland). Time-radioactivity curves were fit using the simplified reference tissue model (SRTM; Lammertsma and Hume 1996); to provide an estimation of k2′, the rate constant for the transfer of the tracer from the reference region to the plasma. As the cerebellum is nearly devoid of specific binding sites for the radiotracer, a cerebellar volume of interest (VOI) was used as a reference region (Mukherjee et al. 2002). A volume-weighted average of k2′ estimates from high-radioactivity regions (i.e., the caudate and putamen) was computed. The time-radioactivity curves were refit using the SRTM2 model (Wu and Carson 2002), with the computed k2′ value held constant across all VOIs. BP_{ND} was then calculated by subtracting 1.0 from the product of the tracer delivery (R1) and the tracer washout (k2′/k2a).

Analysis of fMRI Parameter Estimates, D2/D3 Receptor Availability, and Behavior

The relationships between fMRI parameter estimates, striatal D2/D3 dopamine receptor BP_{ND}, risk-taking behavior following gains and losses, and total earnings were assessed. Parameter estimates (β-values from the whole-brain GLM parametric analysis that correspond to the modulation of activation by pump number) during pump and cash-out events were extracted from VOIs anatomically defined on the basis of a priori hypotheses. The dorsolateral PFC (DLPFC) was sampled as a spherical VOI with a 10-mm radius around the peak voxel (Montreal Neurological Institute, MNI, coordinates: $x = 30$, $y = 36$, $z = 20$) from a cluster previously associated with risk-taking on the BART (Rao et al. 2008). Bilateral caudate, putamen, and nucleus accumbens regions were anatomically derived from the Harvard-Oxford subcortical atlas and were combined to create a VOI of the whole striatum. To ensure

that the correlations with striatal D2/D3 dopamine receptor BP_{ND} were specific to our hypothesized VOIs, we tested the correlation of D2/D3 dopamine receptor BP_{ND} with parameter estimates from the insula and visual cortex, regions that were not hypothesized to have activation correlated with striatal BP_{ND}. VOIs of the insula and visual cortex were anatomically defined from the Harvard-Oxford cortical atlas. To assess pumping behavior that was not limited by a balloon explosion, an adjusted average number of pumps was calculated by dividing the total number of pumps in trials without explosions by the number of such trials. "Risk-taking after reward" was calculated by subtracting the adjusted number of pumps following control-balloon trials from those following cash-out events. "Risk-taking after loss" was calculated as the difference between the adjusted number of pumps following explosion events and following control-balloon trials. Overall performance was defined as total earnings on the BART. Sex and age were entered as covariates for all correlation analyses, and multiple-comparison correction was performed by controlling for the rate of false discoveries (FDR; 5% α-level) (Benjamini and Hochberg 1995).

Results

Behavioral Performance

On average, participants decided to cash out on 52% of all trials (SD = 10.22%) and pumped active balloons 8.48 times (SD = 2.29) across all trials and 2.92 times (SD = 0.97) on trials ending with a choice to cash out. Taking the number of pumps on active balloons as the dependent variable, there were significant main effects of balloon color ($F_{1,\ 1,450} = 38.665$, $P < 0.001$) and previous trial outcome ($F_{1,\ 1,463} = 12.061$, $P = 0.001$); however, there was no significant main effect of the trial number ($F_{88,\ 1,452} = 1.194$, $P = 0.112$). The results also showed no significant interactions between trial number and balloon color ($F_{80,\ 1,455} = 0.664$, $P = 0.990$) or between trial number and previous trial outcome ($F_{76,\ 1,455} = 1.238$, $P = 0.085$). Post hoc analyses showed that participants made significantly fewer pumps on red than blue balloons and on trials following balloon explosion compared with cash-out events ($P < 0.05$).

fMRI Analysis

Modulation of Activation by the Pump Number

Activation in the right inferior and right middle frontal gyri, right orbitofrontal cortex, right insula, anterior cingulate, thalamus, and brainstem was modulated by pump number during active balloon pumps ($P < 0.05$, whole-brain cluster corrected; Fig. 2*a* and Table 1). In cash-out events, activation in nucleus

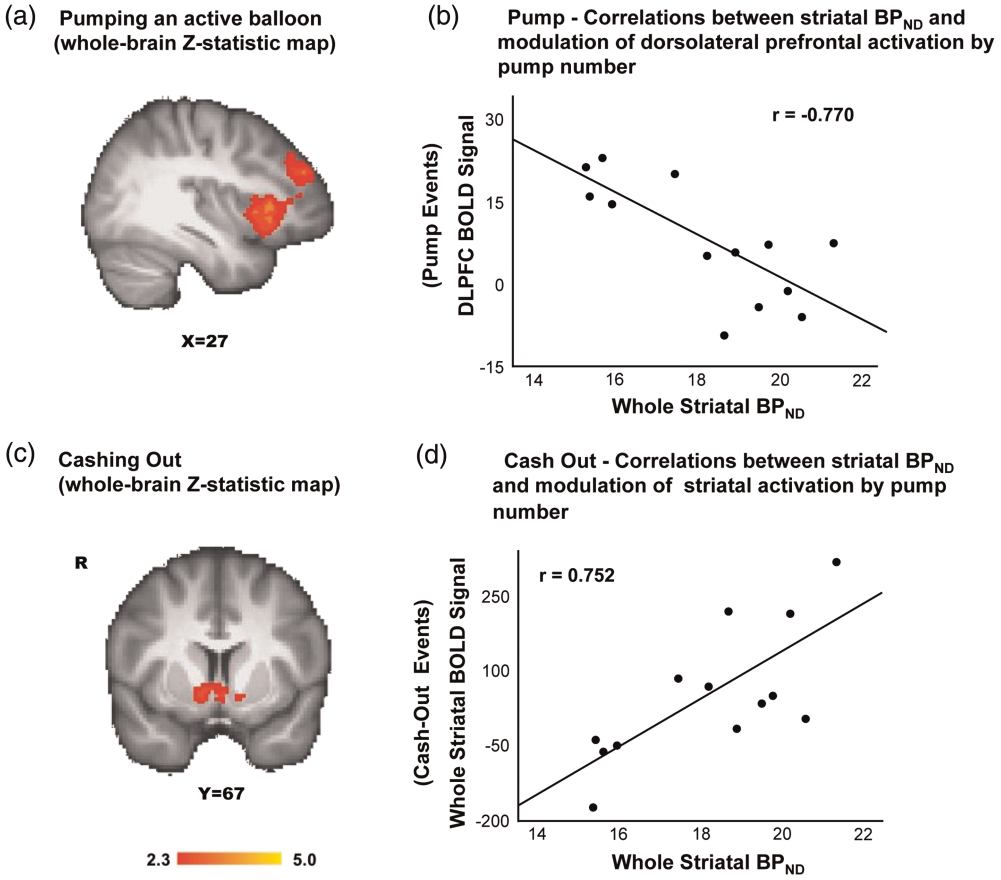

Figure 2. Modulation of striatal and prefrontal cortical activation by pump number and the relationship with striatal BP_{ND}. (*a*) The modulation of activation by pump number was exhibited during active balloon pumps (see Methods for details of parametric modulation analysis) (see Table 1 for the list of regions). (*b*) The fMRI parameter estimates (in β-values) extracted from DLPFC (independently defined VOI) from pump events were negatively correlated with striatal BP_{ND} (*x*-axis). (*c*) In cash-out events, the modulation of activation by pump number was seen in the ventral striatum (see Table 1 for the list of regions). (*d*) The fMRI parameter estimates (in β-values) for the whole striatum (anatomically defined VOI) from cash-out events (*y*-axis) were positively correlated with striatal BP_{ND} (*x*-axis). Color maps represent *Z*-statistic values (whole-brain cluster-corrected).

accumbens, right caudate, subcallosal and precuneus cortices, and parahippocampal and postcentral gyri was modulated by pump number ($P < 0.05$, whole-brain cluster corrected) (Fig. 2*c* and Table 1).

Effects of Loss on Activation During Subsequent Risk-Taking

Activation in the left amygdala, hippocampus, parahippocampal gyrus, posterior cingulate cortex, and precuneus showed greater modulation by pump number during active balloon pumps following a balloon explosion than following a cash-out event number ($P < 0.05$, whole-brain cluster corrected) (Fig. 3 and Table 2). No regions showed greater modulation of activation by pump number during pumping after a cash-out than balloon-explosion event.

Table 1

Brain regions that exhibited activation modulated by the pump number[a] in the pump and cash-out events

Brain region	Cluster size (voxels)	x[b]	y	z	Z-statistic
Contrast: Pumping an active balloon					
Cluster #1[c]	2414				
Occipital cortex (L/R[d])		2	−84	−6	5.52
Cluster #2	1749				
Insula cortex (R)		32	24	−2	5.52
Middle frontal gyrus (R)		38	46	26	4.52
Orbital frontal cortex (R)		30	22	−12	4.51
Inferior frontal gyrus (R)		54	12	4	3.55
Cluster #3	1312				
Anterior cingulate cortex		6	28	28	4.57
Cluster #4	460				
Brainstem		6	−24	−8	3.75
Thalamus		4	−2	0	3.75
Contrast: Cashing out an active balloon					
Cluster #1[c]	1027				
Precuneus cortex (L/R[d])		−14	−58	18	4.05
Cluster #2	980				
Postcentral gyrus (L)		−28	−32	66	4.03
Cluster #3	687				
Nucleus accumbens (L/R)		12	8	−8	3.40
Caudate (R)		10	22	2	3.34
Subcallosal cortex		2	18	−6	3.33

[a]Amplitudes of BOLD responses associated with pumps and cash outs on active balloons were modeled as a function of parametrically varied levels of risk and reward (represented by the pump number) (see Methods). Z-statistic maps were thresholded using cluster-corrected statistics with a height-threshold of $Z > 2.3$ and cluster-forming threshold of $P < 0.05$.

[b]x, y, and z reflect coordinates for peak voxel or for other local maxima in MNI space.

[c]Clusters are numbered and presented in the order of decreasing size.

[d]L or R refers to the left or right hemisphere.

Relationships Between Striatal D2/D3 BP_{ND}, Frontostriatal Activation, and Risk-Taking Behavior

Striatal D2/D3 BP_{ND} and Frontostriatal Activation

The fMRI parameter estimates (β-values from the whole-brain GLM parametric analysis that correspond to the modulation of activation by pump number) extracted from the DLPFC during pump events showed significant negative correlations with D2/D3 BP_{ND} for the whole striatum (Fig. 2*b*). Post hoc analyses showed significant negative correlations with D2/D3 BP_{ND} for the caudate nucleus ($r = -0.911$, $P < 0.001$), putamen ($r = -0.725$, $P = 0.006$), and nucleus accumbens ($r = -0.495$, $P = 0.05$) (FDR corrected). In contrast, fMRI parameter estimates of the whole striatum for cash-out events showed significant positive correlations with whole-striatal D2/D3 BP_{ND} (Fig. 2*d*). Post hoc analyses showed positive correlations with D2/D3 BP_{ND} for the caudate nucleus ($r = 0.600$, $P = 0.025$), putamen ($r = 0.523$, $P = 0.049$), and nucleus accumbens ($r = 0.502$, $P = 0.05$) (FDR uncorrected). There were no significant correlations between striatal D2/D3 BP_{ND} and the fMRI parameter estimates of activation in the control regions: Insula ($r = 0.099$, $P = 0.772$) and visual cortex ($r = 0.269$, $P = 0.424$), demonstrating that the effects were not generalized.

Striatal D2/D3 BP_{ND}, Risk-Taking After Reward or After Loss, and Overall Performance

The number of risky choices that a participant took after a reward (the number of pumps after cash-out trials minus after control trials was negatively correlated with D2/D3 BP_{ND} for the whole striatum; Fig. 4*a*). Post hoc analyses revealed that this correlation was significant for each striatal subregion (caudate, putamen, and nucleus accumbens; $P < 0.011$, FDR corrected; Fig. 4*a*). There were no significant correlations

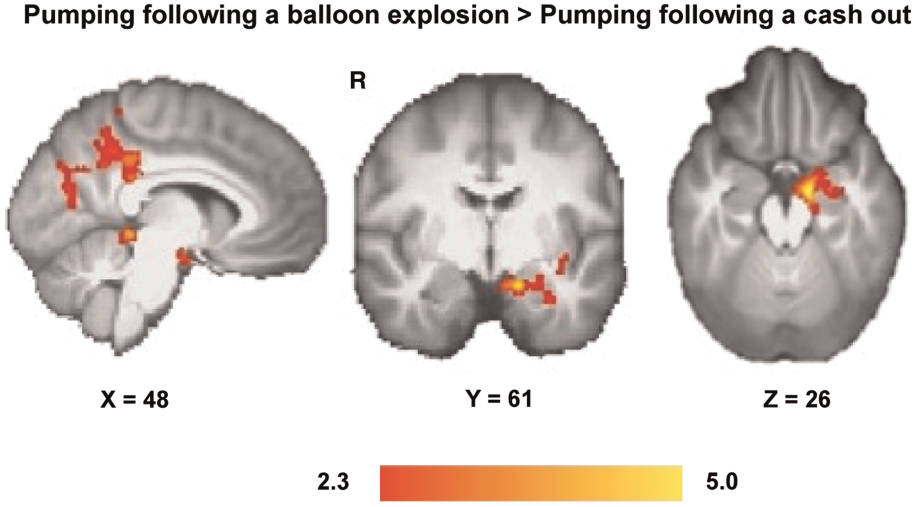

Figure 3. Effect of balloon explosions on the modulation of brain activation by pump number while pumping in subsequent trials. The modulation of activation by pump number was greater in the left amygdala, hippocampus, parahippocampal gyrus, posterior cingulate, and precuneus cortices for pumps after a balloon explosion compared with pumps after cashing out. Color maps represent Z-statistic values (whole-brain cluster-corrected).

between the number of risky choices after a loss (the number of pumps after balloon explosions minus the number of pumps after control trials and striatal D2/D3 BP_{ND}; $r = -0.350$, $P = 0.291$). Overall performance on the BART, measured by total earnings, was negatively correlated with D2/D3 BP_{ND} for the whole striatum and for each subregion; caudate nucleus ($r = -0.645$, $P = 0.016$), putamen ($r = -0.555$, $P = 0.038$), and nucleus accumbens ($r = -0.633$, $P = 0.018$) (FDR uncorrected; Fig. 5*a*).

Table 2

Brain regions that exhibited greater modulation of activation by the pump number[a] in pump events following a balloon explosion compared with after a cash-out event

Brain region	Cluster size (voxels)	x[b]	y	z	Z-statistic
Contrast: Pumping following an explosion > pumping following a cash out					
Cluster #1[c]	946				
Posterior cingulate cortex (L[d])		−8	−38	36	3.38
Cluster #2	767				
Hippocampus (L)		−14	−8	−20	3.83
Amygdala (L)		−16	−4	−20	3.78
Parahippocampal gyrus (L)		−16	−28	−14	3.38

[a]Amplitudes of BOLD responses associated with pumps on active balloons were modeled as a function of parametrically varied levels of risk and reward (represented by the pump number) (see Methods). Z-statistic maps were thresholded using cluster-corrected statistics with a height-threshold of $Z > 2.3$ and cluster-forming threshold of $P < 0.05$.
[b]x, y, and z reflect coordinates for peak voxel or for other local maxima in MNI space.
[c]Clusters are numbered and presented in the order of decreasing size.
[d]L or R refers to the left or right hemisphere.

Frontostriatal Activation, Risk-Taking After Reward or After Loss, and Overall Performance

The number of risky choices after a reward was also negatively correlated with fMRI parameter estimates for cash-out events for the whole striatum (Fig. 4*b*). Post hoc analyses showed significant negative correlations for the caudate nucleus and putamen ($P < 0.03$, FDR corrected; Fig. 4*b*). In the larger sample ($n = 60$), the number of risky choices after a reward was also negatively correlated with fMRI parameter estimates for cash-out events for the whole striatum and each striatal subregion ($P < 0.05$). There were no significant correlations between the number of risky choices after a loss (the number of pumps after balloon explosions minus the number of pumps after control trials) and striatal fMRI parameter estimates for cash-out events ($r = -0.388$, $P = 0.238$). Total earnings, which was negatively correlated with striatal D2/D3 BP_{ND}, was positively correlated with DLPFC fMRI parameter estimates for pump events ($n = 13$: $r = 0.545$, $P = 0.005$, $n = 60$; $r = 0.200$, $P = 0.06$; Fig. 5*b*).

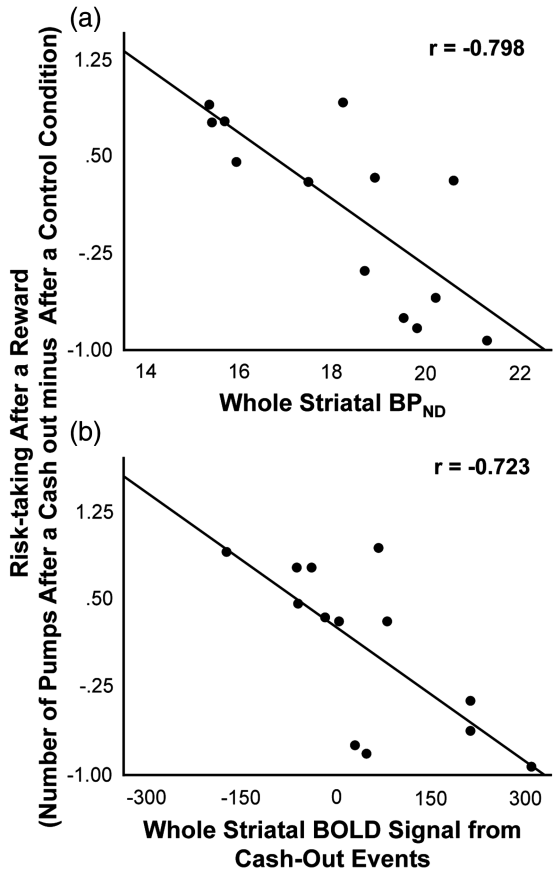

Correlations between BP_{ND} in striatal regions and risk-taking behavior after reward

Striatal Regions	Correlation Coefficient	Significance
Whole Striatum	r = -0.798	p = 0.002*
Caudate Nucleus	r = -0.681	p = 0.011*
Putamen	r = -0.730	p = 0.005*
Nucleus Accumbens	r = -0.845	p = 0.001*

Correlations between striatal BOLD of cash-out events and risk-taking behavior after reward

Striatal Regions	Correlation Coefficient	Significance
Whole Striatum	r = -0.723	p = 0.006*
Caudate Nucleus	r = -0.758	p = 0.003*
Putamen	r = -0.597	p = 0.026*
Nucleus Accumbens	r = -0.415	p = 0.102

Figure 4. Relationship between risk-taking after a reward, striatal BP_{ND}, and modulation of striatal fMRI activation. Shown are scatter plots, correlation coefficients (r), and associated significance values (P) from post hoc Pearson's correlations. (*a*) Risk-taking after a reward was negatively correlated with striatal BP_{ND}. (*b*) Negative relationship between the modulation of striatal activation by pump number in cash-out events and risk-taking in subsequent trials. Risk-taking after a reward was the difference between the number of pumps following trials that ended in a cash-out and those following control trials. Results were controlled for age and sex and remained significant (*) after correcting for the number of tests by controlling the FDR. There were no significant correlations between the difference in the number of pumps after an explosion and the number of pumps after control trials and BP_{ND} in the striatum or striatal parameter estimates.

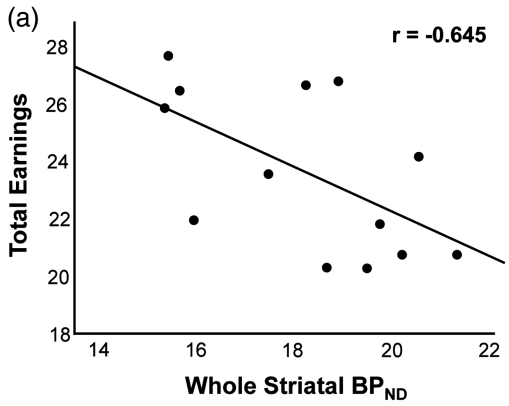

Correlations between BP_{ND} in striatal regions and total earnings

Striatal Regions	Correlation Coefficient	Significance
Whole Striatum	r = -0.645	p = 0.016
Caudate Nucleus	r = -0.555	p = 0.038
Putamen	r = -0.504	p = 0.057
Nucleus Accumbens	r = -0.633	p = 0.018

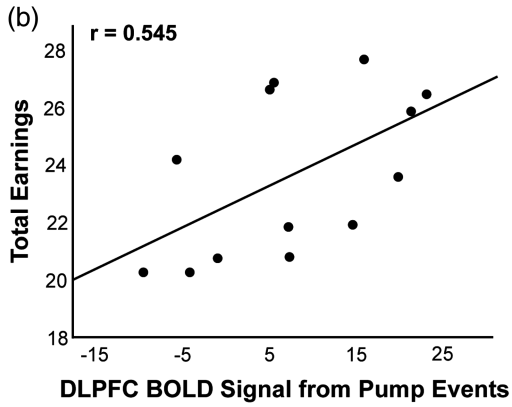

Figure 5. Relationship between BART performance, striatal BP_{ND}, and modulation of DLPFC activation by pump number. (*a*) Total earned on the BART was negatively correlated with striatal BP_{ND}. Shown are correlation coefficients (*r*) and associated significance values (*P*) from post hoc Pearson's correlations for the relationship between total earnings on the BART and striatal BP_{ND} for each striatal subregion. (*b*) The modulation of the DLPFC activation by pump number in pump events showed a positive relationship with amount earned on the BART ($P = 0.005$). Results are controlled for age and sex.

Discussion

The findings reported here show that the outcomes of previous decisions, striatal D2/D3 BP_{ND}, and modulation of frontal and subcortical activation are all associated with risky decision-making. Presenting direct evidence for the involvement of striatal D2/D3 receptors in risk-taking behavior, our results extend previous findings of frontostriatal activation in decision-making (Ernst and Paulus 2005; Krain et al. 2006; Rao et al. 2008) and suggest a potential mechanism by which striatal dopamine may modulate frontal and striatal regions during risky choices.

The findings indicate that risky decision-making is, in part, associated with previous trial outcomes. Participants took fewer risks when the preceding trial resulted in a loss rather than a gain, consistent with reports that prior outcomes biased decision-making (Leland and Paulus 2005; Mata et al. 2012). Greater modulation of activation in the amygdala, by pump number, following a loss than after a gain suggests that amygdala signaling attenuates risky behavior following aversive outcomes. This view is in line with observations that loss-aversion behavior is positively correlated with amygdala activation in a risky monetary-choice task (Sokol-Hessner et al. 2012), and that patients with amygdala lesions are less loss-averse than healthy controls (De Martino et al. 2010). Although our results confirm the involvement of the insula during risky decision-making (Paulus et al. 2003), the lack of insula activation related to previous trial outcomes suggests that the insula is insensitive to recent experience. The hippocampus, which is implicated in encoding recent experiences (Ferbinteanu and Shapiro 2003), showed a greater response after a loss than after a win. Given the involvement of the hippocampus in processing associations among different experiences (Burgess et al. 2002) and of the amygdala in promoting cautious behavior in uncertain situations (Mason et al. 2006), the results suggest a neural mechanism by which recent losses promote risk aversion by signaling the potential for further negative outcomes and by guiding subsequent choices accordingly.

Our results also highlight the importance of rewarding experiences in shaping behavior. The modulation of striatal activation by pump number during the cash-out condition was related to striatal D2/D3 BP_{ND}, and both predicted risk-taking behavior on the subsequent trial. These results are consistent with prior observations that ventral striatal activation (Knutson et al. 2001) and firing in dopaminergic neurons (Tobler et al. 2005) are related to the magnitude of anticipated reward. It has been suggested that anticipatory responses of the dopamine system promote reinforcement learning (Schultz 1998) and modulate risk preferences (St Onge and Floresco 2009; Sugam et al. 2012). It has also been observed that D2/D3 receptor agonists enhance reward-expectancy signaling via dopaminergic transmission (Winstanley et al. 2011) and reduce risky choices (Simon et al. 2011). We extend these findings by showing that

striatal D2/D3 BP_{ND} is directly related to striatal activation during reward-seeking behavior that involves risk in humans.

Risky decisions are determined, in part, by motivational states that reflect activity in the ventral striatum (Salamone et al. 2005) and by assessment and maintenance of goal states supported by PFC activity (Ridderinkhof et al. 2004). Pharmacological studies in rodents have demonstrated a crucial role of striatal dopamine in the adaptation of these processes by the flexible updating of reinforcement contingencies (Seamans and Yang 2004; Cools and D'Esposito 2011). The PFC and striatum interact through an elaborate system of interconnections (Cummings 1995; Sesack and Grace 2010) that likely contributes to goal-directed states. In the context of decision-making involving risk and reward, these interactions may be described in a framework (described below) in which reinforcement values are reflected in activity-dependent plasticity that is governed by differences in striatal D2/D3 receptor BP_{ND}. Such changes can effectively bias decisions in favor of reward-seeking or goal-directed behavior.

Corticostriatal computational models show a modulatory role of the PFC on striatal activity (Doll et al. 2009; Frank 2011). The PFC can influence striatal activity through various signaling pathways including mesocortical glutamatergic projections that enhance tonic striatal dopamine release, which, in turn, increases the effective threshold for striatal firing (Grace 1991; Frank et al. 2001), other corticostriatal projections that enhance non-AMPA-mediated glutamatergic synaptic transmission (Cepeda et al. 1992, 1993; Levine and Cepeda 1998), and a cortico-subthalamic-striatal hyperdirect pathway that has been implicated in inhibiting premature responses in high-conflict situations (Frank 2006, 2011). As presynaptic striatal D2/D3 receptors play a critical role in inhibiting glutamate release in these pathways (Cepeda et al. 2001; Gonzalez et al. 2012), striatal D2/D3 receptor availability may thereby determine the extent to which PFC activity and associated glutamate release can activate GABAergic striatal neurons to inhibit activity and maintain goal-directed behavior.

While presynaptic D2/D3 receptors can limit prefrontal influence over striatal activity (Cepeda et al. 2001), postsynaptic striatal D2/D3 receptor activation can attenuate the spiking of prefrontal neurons (Seamans and Yang 2004). Postsynaptic striatal D2/D3 receptor activation can indirectly disinhibit the dorsomedial nucleus of the thalamus through afferents to the ventral pallidum or substantia nigra pars reticulata, which both provide inhibitory inputs to GABAergic inhibitory neurons in the thalamus (Montaron et al. 1996; Sesack and Grace 2010). As the disinhibition of the dorsomedial nucleus of the thalamus results in the excitation of prefrontal pyramidal neurons that have been implicated in motivational states, striatal D2/D3 receptor activation has the capacity to modify goal-directed behavior governed by the PFC (Cohen et al. 1996; Frank 2011).

Since presynaptic and postsynaptic striatal D2/D3 receptors affect glutamatergic and GABAergic signaling in the striatum (Seamans and Yang 2004), D2/D3 receptor availability may contribute to changes in the computational properties of frontostriatal circuits during risky decision-making. Supporting this view is our observation that participants with low D2/D3 BP_{ND} exhibited less ventral striatal response to reward, but greater modulation of DLPFC activation while pumping and better performance on the BART. Given that lesions to corticostriatal projections shift decisions related to reward contingencies in rodents (St Onge et al. 2012) and neurocomputational models suggest that PFC activity can directly override striatal representations of the reinforcement value (Doll et al. 2009), the inverse relationship between ventral striatal activation when taking reward and DLPFC activation when taking risk may reflect corticostriatal regulation of reward-driven responses through D2-receptor-mediated effects on glutamate release.

Individuals with high D2/D3 BP_{ND} exhibited both greater reward-driven activation in the ventral striatum and more immediate reward-seeking behavior following reward than counterparts with low D2/D3 BP_{ND}. The results suggest that individuals with high striatal D2/D3 receptor BP_{ND} are more sensitive to reward and have less-effective cortical inhibition of reward-driven responses that lead to a preference for immediate smaller gains over potentially larger delayed ones. Striatal D2/D3 receptors may thereby determine the capacity to respond to striatal dopamine release that signals for imminent reward, and this signal, in turn, would update reinforcement values represented in the PFC. The results presented here, however, are inconsistent with the observation that stimulant-dependent individuals, who exhibit low striatal BP_{ND} (Volkow et al. 2001), exhibit temporal discounting of rewards (Monterosso et al. 2007). One possible explanation is that there is a nonlinear relationship between dopaminergic function and temporal discounting of rewards, as suggested by the observation that low doses of amphetamine significantly increased the preference for rats to work harder or to wait longer for larger rewards, while high doses had the opposite effect (Floresco et al. 2008). Our findings may reflect the descending limb of an inverted U-shaped function that describes the relationship between dopamine function and adaptive risky decision-making, although small sample size and limited dynamic range in binding potentials prevent definitive interpretation. In view of the preceding discussion, it is plausible that individual differences in striatal D2/D3 receptors that contribute to individual differences in reward sensitivity (Cohen et al. 2005) may determine variation in goal-directed behavior and associated modulation of frontal and striatal activation. This may be accomplished by facilitating or inhibiting glutamate and dopamine release in various signaling pathways linking the striatum and PFC.

This study has some limitations. The combination of the temporal resolution of fMRI with the BART was not sufficient to allow clear dissociation between the decision to cash out and receipt of reward. Thus, activation related to cash-out events reflects both decision processes and reward receipt. In addition, as potential earnings and the risk of forfeiting earnings increased in tandem with each pump, it was not possible to discern whether the level of risk or reward modulated the activation. Since striatal activation has been observed in the response to both aversive (Jensen et al. 2003) and rewarding (Knutson et al. 2001) stimuli, the modulation of activation of the ventral striatum during cash-out events may reflect anticipation of an aversive outcome (balloon explosion) and not only expectation of reward. Therefore, caution should be taken when attempting to assign function to brain activations via reverse inference (Poldrack 2006).

Despite these limitations, our results not only corroborate, but also extend previous findings of activation in frontostriatal regions during decision-making by highlighting the molecular basis of such activation. They strengthen support for the role

of dopamine in risky decision-making by showing that D2/D3 receptor availability is associated with risky choices as well as the risk sensitivity of a relevant frontostriatal network during decision-making. This study provides evidence that the neural substrates of decision-making vary as a function of individual differences in the striatal dopamine system and the context in which decisions are made.

Funding

The research described here was funded in part by NIH grants P20 DA022539 and R01 DA020726, a grant from Philip Morris USA, and endowments from the Thomas P. and Katherine K. Pike Chair in Addiction Studies, and the Marjorie M. Greene Trust. M.K., A.M.M., and C.L.R. were supported by training grant T32 DA 024635. M.K. and A.M.M. were also supported by NIH grants F31 DA033120-02 and F31 DA0331-17, respectively. None of the sponsors were involved with the design, collection, analysis or interpretation of data, writing the manuscript, or the decision to submit the manuscript for publications.

Notes

Conflict of Interest: None declared.

References

Andersson J, Jenkinson M, Smith S. 2007. Non-linear registration, aka Spatial normalisation in FMRIB technical report.

Ardekani BA, Braun M, Hutton BF, Kanno I, Iida H. 1995. A fully automatic multimodality image registration algorithm. J Comput Assist Tomogr. 19:615–623.

Bechara A, Damasio H, Tranel D, Anderson SW. 1998. Dissociation of working memory from decision making within the human prefrontal cortex. J Neurosci. 18:428–437.

Benjamini Y, Hochberg Y. 1995. Controlling the false discovery rate - a practical and powerful approach to multiple testing. J R Stat Soc Ser B Method. 57:289–300.

Berntson GG, Norman GJ, Bechara A, Bruss J, Tranel D, Cacioppo JT. 2011. The insula and evaluative processes. Psychol Sci. 22:80–86.

Buchel C, Holmes AP, Rees G, Friston KJ. 1998. Characterizing stimulus-response functions using nonlinear regressors in parametric fMRI experiments. NeuroImage. 8:140–148.

Burgess N, Maguire EA, O'Keefe J. 2002. The human hippocampus and spatial and episodic memory. Neuron. 35:625–641.

Cepeda C, Buchwald NA, Levine MS. 1993. Neuromodulatory actions of dopamine in the neostriatum are dependent upon the excitatory amino acid receptor subtypes activated. Proc Natl Acad Sci USA. 90:9576–9580.

Cepeda C, Hurst RS, Altemus KL, Flores-Hernandez J, Calvert CR, Jokel ES, Grandy DK, Low MJ, Rubinstein M, Ariano MA et al. 2001. Facilitated glutamatergic transmission in the striatum of D2 dopamine receptor-deficient mice. J Neurophysiol. 85:659–670.

Cepeda C, Radisavljevic Z, Peacock W, Levine MS, Buchwald NA. 1992. Differential modulation by dopamine of responses evoked by excitatory amino acids in human cortex. Synapse. 11:330–341.

Cohen JD, Braver TS, O'Reilly RC. 1996. A computational approach to prefrontal cortex, cognitive control and schizophrenia: recent developments and current challenges. Philos Trans R Soc Lond B Biol Sci. 351:1515–1527.

Cohen MX, Young J, Baek JM, Kessler C, Ranganath C. 2005. Individual differences in extraversion and dopamine genetics predict neural reward responses. Brain Res Cogn Brain Res. 25:851–861.

Cools R, D'Esposito M. 2011. Inverted-U-shaped dopamine actions on human working memory and cognitive control. Biol Psychiatry. 69: e113–e125.

Cummings JL. 1995. Anatomic and behavioral aspects of frontal-subcortical circuits. Ann N Y Acad Sci. 769:1–13.

Dayan P, Daw ND. 2008. Decision theory, reinforcement learning, and the brain. Cogn Affect Behav Neurosci. 8:429–453.

De Martino B, Camerer CF, Adolphs R. 2010. Amygdala damage eliminates monetary loss aversion. Proc Natl Acad Sci USA. 107:3788–3792.

Doll BB, Jacobs WJ, Sanfey AG, Frank MJ. 2009. Instructional control of reinforcement learning: a behavioral and neurocomputational investigation. Brain Res. 1299:74–94.

Ernst M, Paulus MP. 2005. Neurobiology of decision making: a selective review from a neurocognitive and clinical perspective. Biol Psychiatry. 58:597–604.

Ferbinteanu J, Shapiro ML. 2003. Prospective and retrospective memory coding in the hippocampus. Neuron. 40:1227–1239.

Fitzmaurice GM, Laird NM, Ware JH. 2004. Applied longitudinal analysis. Hoboken (NJ): John Wiley.

Floresco SB, Tse MT, Ghods-Sharifi S. 2008. Dopaminergic and glutamatergic regulation of effort- and delay-based decision making. Neuropsychopharmacology. 33:1966–1979.

Frank MJ. 2011. Computational models of motivated action selection in corticostriatal circuits. Curr Opin Neurobiol. 21:381–386.

Frank MJ. 2006. Hold your horses: a dynamic computational role for the subthalamic nucleus in decision making. Neural Netw. 19:1120–1136.

Frank MJ, Loughry B, O'Reilly RC. 2001. Interactions between frontal cortex and basal ganglia in working memory: a computational model. Cogn Affect Behav Neurosci. 1:137–160.

Gold JI, Shadlen MN. 2007. The neural basis of decision making. Annu Rev Neurosci. 30:535–574.

Gonzalez S, Rangel-Barajas C, Peper M, Lorenzo R, Moreno E, Ciruela F, Borycz J, Ortiz J, Lluis C, Franco R et al. 2012. Dopamine D4 receptor, but not the ADHD-associated D4.7 variant, forms functional heteromers with the dopamine D2S receptor in the brain. Mol Psychiatry. 17:650–662.

Grace AA. 1991. Phasic versus tonic dopamine release and the modulation of dopamine system responsivity: a hypothesis for the etiology of schizophrenia. Neuroscience. 41:1–24.

Jenkinson M, Bannister P, Brady M, Smith S. 2002. Improved optimization for the robust and accurate linear registration and motion correction of brain images. Neuroimage. 17:825–841.

Jensen J, McIntosh AR, Crawley AP, Mikulis DJ, Remington G, Kapur S. 2003. Direct activation of the ventral striatum in anticipation of aversive stimuli. Neuron. 40:1251–1257.

Kahneman D, Tversky A. 1984. Choices, values, and frames. Am Psycholog. 39:341–350.

Knutson B, Adams CM, Fong GW, Hommer D. 2001. Anticipation of increasing monetary reward selectively recruits nucleus accumbens. J Neurosci. 21:RC159.

Krain AL, Wilson AM, Arbuckle R, Castellanos FX, Milham MP. 2006. Distinct neural mechanisms of risk and ambiguity: a meta-analysis of decision-making. NeuroImage. 32:477–484.

Laird NM. 1988. Missing data in longitudinal studies. Stat Med. 7: 305–315.

Lammertsma AA, Hume SP. 1996. Simplified reference tissue model for PET receptor studies. Neuroimage. 4:153–158.

Lejuez CW, Read JP, Kahler CW, Richards JB, Ramsey SE, Stuart GL, Strong DR, Brown RA. 2002. Evaluation of a behavioral measure of risk taking: the Balloon Analogue Risk Task (BART). J Exp Psychol Appl. 8:75–84.

Leland DS, Paulus MP. 2005. Increased risk-taking decision-making but not altered response to punishment in stimulant-using young adults. Drug Alcohol Depend. 78:83–90.

Levine MS, Cepeda C. 1998. Dopamine modulation of responses mediated by excitatory amino acids in the neostriatum. Adv Pharmacol. 42:724–729.

Little RJA, Rubin DB. 2002. Statistical analysis with missing data. 2nd ed. New York: John Wiley.

Mason WA, Capitanio JP, Machado CJ, Mendoza SP, Amaral DG. 2006. Amygdalectomy and responsiveness to novelty in rhesus monkeys (*Macaca mulatta*): generality and individual consistency of effects. Emotion. 6:73–81.

Mata R, Hau R, Papassotiropoulos A, Hertwig R. 2012. DAT1 polymorphism is associated with risk taking in the Balloon Analogue Risk Task (BART). PLoS One. 7:e39135.

Montaron MF, Deniau JM, Menetrey A, Glowinski J, Thierry AM. 1996. Prefrontal cortex inputs of the nucleus accumbens-nigro-thalamic circuit. Neuroscience. 71:371–382.

Monterosso JR, Ainslie G, Xu J, Cordova X, Domier CP, London ED. 2007. Frontoparietal cortical activity of methamphetamine-dependent and comparison subjects performing a delay discounting task. Hum Brain Mapp. 28:383–393.

Mukherjee J, Christian BT, Dunigan KA, Shi B, Narayanan TK, Satter M, Mantil J. 2002. Brain imaging of 18F-fallypride in normal volunteers: blood analysis, distribution, test-retest studies, and preliminary assessment of sensitivity to aging effects on dopamine D-2/D-3 receptors. Synapse. 46:170–188.

Mukherjee J, Yang ZY, Das MK, Brown T. 1995. Fluorinated benzamide neuroleptics—III. Development of (S)-N-[(1-allyl-2-pyrrolidinyl) methyl]-5-(3-[18F]fluoropropyl)-2, 3-dimethoxybenzamide as an improved dopamine D-2 receptor tracer. Nucl Med Biol. 22:283–296.

Niv Y, Edlund JA, Dayan P, O'Doherty JP. 2012. Neural prediction errors reveal a risk-sensitive reinforcement-learning process in the human brain. J Neurosci. 32:551–562.

Paulus MP, Rogalsky C, Simmons A, Feinstein JS, Stein MB. 2003. Increased activation in the right insula during risk-taking decision making is related to harm avoidance and neuroticism. NeuroImage. 19:1439–1448.

Poldrack RA. 2006. Can cognitive processes be inferred from neuroimaging data? Trends Cogn Sci. 10:59–63.

Rao H, Korczykowski M, Pluta J, Hoang A, Detre JA. 2008. Neural correlates of voluntary and involuntary risk taking in the human brain: an fMRI study of the Balloon Analog Risk Task (BART). NeuroImage. 42:902–910.

Ridderinkhof KR, Ullsperger M, Crone EA, Nieuwenhuis S. 2004. The role of the medial frontal cortex in cognitive control. Science. 306:443–447.

Salamone JD, Correa M, Mingote SM, Weber SM. 2005. Beyond the reward hypothesis: alternative functions of nucleus accumbens dopamine. Curr Opin Pharmacol. 5:34–41.

Schott BH, Minuzzi L, Krebs RM, Elmenhorst D, Lang M, Winz OH, Seidenbecher CI, Coenen HH, Heinze HJ, Zilles K et al. 2008. Mesolimbic functional magnetic resonance imaging activations during reward anticipation correlate with reward-related ventral striatal dopamine release. J Neurosci. 28:14311–14319.

Schultz W. 1998. Predictive reward signal of dopamine neurons. J Neurophysiol. 80:1–27.

Seamans JK, Yang CR. 2004. The principal features and mechanisms of dopamine modulation in the prefrontal cortex. Prog Neurobiol. 74:1–58.

Sesack SR, Grace AA. 2010. Cortico-basal ganglia reward network: microcircuitry. Neuropsychopharmacology. 35:27–47.

Simon NW, Montgomery KS, Beas BS, Mitchell MR, LaSarge CL, Mendez IA, Banuelos C, Vokes CM, Taylor AB, Haberman RP et al. 2011. Dopaminergic modulation of risky decision-making. J Neurosci. 31:17460–17470.

Sokol-Hessner P, Camerer CF, Phelps EA. 2012. Emotion regulation reduces loss aversion and decreases amygdala responses to losses. Soc Cogn Affect Neurosci. 8:341–350.

St Onge JR, Floresco SB. 2009. Dopaminergic modulation of risk-based decision making. Neuropsychopharmacology. 34:681–697.

St Onge JR, Stopper CM, Zahm DS, Floresco SB. 2012. Separate prefrontal-subcortical circuits mediate different components of risk-based decision making. J Neurosci. 32:2886–2899.

Sugam JA, Day JJ, Wightman RM, Carelli RM. 2012. Phasic nucleus accumbens dopamine encodes risk-based decision-making behavior. Biol Psychiatry. 71:199–205.

Tobler PN, Fiorillo CD, Schultz W. 2005. Adaptive coding of reward value by dopamine neurons. Science. 307:1642–1645.

Volkow ND, Chang L, Wang GJ, Fowler JS, Ding YS, Sedler M, Logan J, Franceschi D, Gatley J, Hitzemann R et al. 2001. Low level of brain dopamine D2 receptors in methamphetamine abusers: association with metabolism in the orbitofrontal cortex. Am J Psychiatry. 158:2015–2021.

Winstanley CA, Cocker PJ, Rogers RD. 2011. Dopamine modulates reward expectancy during performance of a slot machine task in rats: evidence for a 'near-miss' effect. Neuropsychopharmacology. 36:913–925.

Wu Y, Carson RE. 2002. Noise reduction in the simplified reference tissue model for neuroreceptor functional imaging. J Cereb Blood Flow Metab. 22:1440–1452.